

# Effects of Fuel Nozzle Geometry on the Flammability Limits of Low-Swirl Biogas Diffusion Flames

S. C. Fabbro and M. Birouk

Department of Mechanical Engineering, University of Manitoba  
15 Gillson St., Winnipeg, Manitoba, Canada R3T 5V6

## 1 Introduction

The global dependence on combustion for energy production is integrated into so many aspects of modern society including power generation, heating, and transportation. Rising energy demands and concerns over greenhouse gas (GHG) emissions, particularly their impact on climate change, have accelerated the shift toward renewable energy sources. Biologically sourced fuels, compatible with existing infrastructure, offer a quick and practical transition away from fossil fuels. Among these, biogas stands out as a viable substitute for fossil-based gaseous fuels like natural gas. Biogas, primarily composed of methane ( $\text{CH}_4$ ) and carbon dioxide ( $\text{CO}_2$ ), is produced through anaerobic decomposition of organic materials such as agricultural residues, municipal waste, sewage, and food waste [2,3]. Biogas is a carbon-neutral fuel with significant potential to mitigate GHG emissions. Its combustion replaces fossil fuel-derived carbon dioxide and prevents methane emissions from decomposing organic materials. This is particularly impactful given methane's global warming potential, which is 28 to 36 times greater than  $\text{CO}_2$  over a 100-year horizon (IPCC, 2014). Thus, biogas use offers dual environmental benefits by reducing both short- and long-term GHG effects. However, the use of biogas as a fuel faces challenges due to its low energy density and weak flame stability. Methane, the combustible component, is heavily diluted by inert  $\text{CO}_2$ , which reduces the adiabatic flame temperature, burning velocity, and flammability range [5,7]. Carbon dioxide also disrupts chemical kinetics and lowers thermal energy availability, compounding these limitations. Even at concentrations lower than typical biogas levels,  $\text{CO}_2$  significantly restricts conditions for stable combustion, Hwang et al. [4]. Leung et al. [6] found that biogas flames exhibit blowoff limits 6 to 7 times lower and lift-off heights 4 times smaller than methane flames, underscoring the impact of  $\text{CO}_2$  dilution on flame stability. Addressing these limitations requires advancements in burner design and flow dynamics. Saediamiri et al. [1] demonstrated that optimizing burner geometries and incorporating swirling flows significantly enhance flame stability by promoting heat and reactive species recirculation. Further research by Saediamiri et al. [12] revealed that while higher  $\text{CO}_2$  levels narrow flammability ranges and reduce flame speeds, these issues can be mitigated through optimized burner geometries and enhanced

mixing. These findings emphasize the critical importance of burner design and flow optimization in overcoming biogas combustion challenges, paving the way for its broader adoption as a sustainable fossil fuel alternative. Bluff bodies are widely recognized for their ability to induce vortex formation in their wake, thereby enhancing turbulence, promoting efficient mixing, and contributing to flame stabilization in combustion systems, Tong et al. [10]. The present study investigates the effect of fuel nozzle geometry on the stability of a low-swirl non-premixed biogas flame. Specifically, the focus is on bluff bodies with a pronounced lip thickness of the fuel nozzle, a design feature expected to facilitate the formation of a lower recirculation zone that promotes flame anchoring and improved overall combustion stability, Khalladi et al. [11].

## 2 Methodology

The experimental setup for the bluff-body and non-bluff body fuel nozzle configurations is shown in Figure 1a and 1b, respectively. Both the swirling co-airflow and concentric fuel nozzle discharge into an enclosed atmospheric combustion chamber. For both fuel nozzle configurations, the co-flow air stream passes through an axial swirl generator equipped with vanes angled at  $30^\circ$ , corresponding to a geometrical swirl number ( $S$ ) of 0.39. The co-airflow exit area was maintained at  $886 \text{ mm}^2$  for both burner geometries. A schematic representation of the burner's upper section for both configurations are shown in Figure 1, including the fuel nozzle (in green color) and swirl generator (in blue color). The fuel nozzle, for both configurations, has an exit diameter of 3.75 mm. A detailed description of the fuel metering system is available in Saediamiri et al. [1] and not included in this abstract for brevity. To ensure uniform mixing of the biogas components prior to combustion, a 600 mm-long cyclone-type mixing pipe was positioned upstream of the fuel nozzle. The biogas fuel surrogate mixture consists of 40%  $\text{CO}_2$  and 60%  $\text{CH}_4$  by volume, and it is maintained fixed throughout all experiments. The procedure for determining the lower fuel limit of the biogas flame stability map involved producing a flame at a stable operating point and then incrementally increasing the volumetric flow rate of the co-airflow at a constant fuel flow until the occurrence of flame blowout. For the upper fuel limit, the co-airflow was gradually decreased until the flame was extinguished. Stability limits were determined by averaging the results of several tests at the same conditions, typically four to five tests under identical conditions, yielding a repeatability within  $\pm 5\%$ . The flow field was characterized using a two-dimensional Dantec Dynamics PIV (Particle Image Velocimetry) system, which captured 1,000 pairs of instantaneous images for each test condition. A comprehensive description of the PIV system is detailed in Saediamiri et al. [1]. The instantaneous PIV images were processed using adaptive correlation with a  $32 \times 32$ -pixel interrogation area and a 50% overlap window. Subsequently, the PIV data was exported for post-processing in MATLAB to analyze the flow field characteristics.

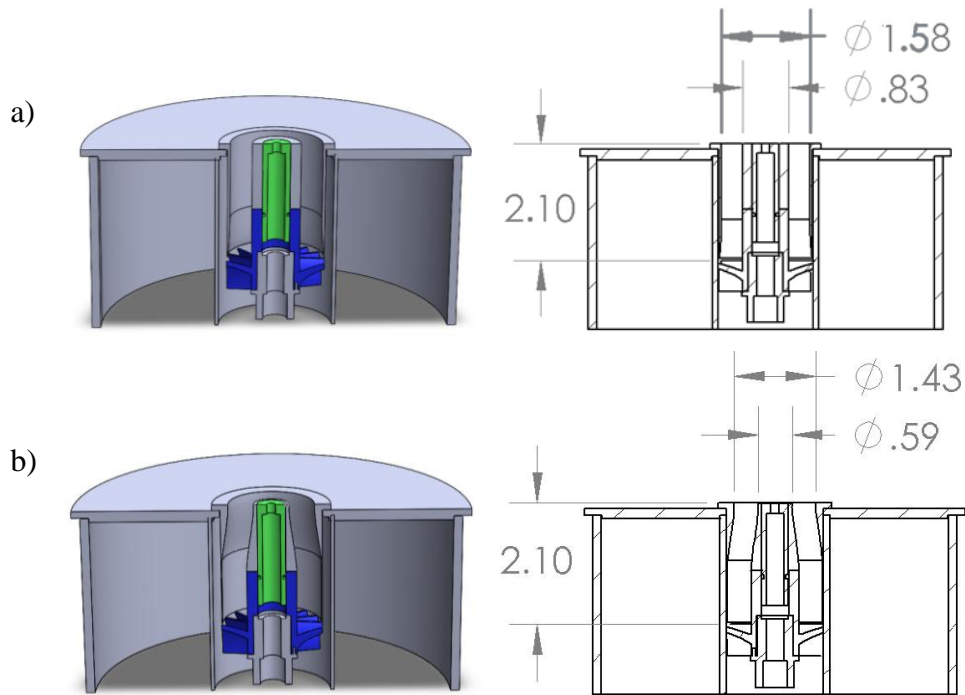


Figure 1. Schematic diagram of the upper burner setup; a) bluff body burner, and b) non-bluff body burner assembly

### 3 Results

Figure 2 presents the flammability map for both burner configurations. The upper flame stability limit (dashed lines) represents the highest fuel flow for a given co-airflow, and the lower stability limit (solid lines) represents the lowest fuel flow for a given co-flow. The stability map for the bluff body (BB) configuration is identified by the square-symbol, and the non-bluff body (NBB) configuration by the triangular-symbol. This figure clearly shows differences in the stability limits between the two burner configurations. The upper limit seems to be largely similar for both burner geometries. However, there is a significant difference in the lower limit. It shows that while the two configurations display similar limits at roughly 10 SLPM of fuel flow, the bluff body configuration of the burner has a significantly larger lower limit below the 10 SLPM fuel flow and a pronounced shrinkage in the lower limit for fuel flow rates higher than 10 SPLM. For both burner configurations, there exist transitions between different types of flames within the stability map. For both fuel nozzle geometry configurations, generally at low fuel rate and co-airflow velocity, the stable flame is attached (flame image i), while it is lifted (flame image iii) at higher fuel flow rates and co-airflow velocities. However, another type of split flame exists for the bluff body configuration (flame image ii). Figure 2 clearly shows that, below the 10 SLPM fuel flow rate, the flame stability range is much extended for the bluff body burner configuration, whereas it is the non-bluff body burner that has larger stability limit for fuel flow rates higher than 10 SLPM.

Figure 3 is presented here as an example of the difference in the flow dynamics of a stable flame between the two burner configurations. This figure is for a stable flame at identical flow conditions which are closer to the lower limit of the bluff body burner (BB) and still far away

from that of non-bluff body (NBB) configuration. Clearly Figure 3a reveals that the presence of lower recirculation zones (LRZ) which are induced due to the existence of a large lip (termed here as bluff body) of the fuel nozzle. Figure 3b, on the other hand, shows no such recirculation. Another very important observation that can be made when comparing Figure 3a to 3b is that the large inner recirculation zone (IRZ) where the flame occurs is much closer to the burner for the non-bluff body burner. The flame is stabilized within this IRZ, which is characterized by very low flow velocities. The presence of the flame closer to the nozzle results in the expansion of the flow field and consequently a faster fuel jet velocity decay, hence a more stable lifted flame. This is in line with the findings of Saediamiri et al. [12] where they used the same nozzle with a tangential low-swirl burner and burned methane instead of biogas. This also helps to explain why for the higher fuel flow rates of the non-bluff body configuration is able to handle higher co-airflow velocities than the bluff body burner. These results help illustrate that changes in burner configuration can indeed alter flame stability and mitigate some of the instabilities inherent in biogas combustion. To further support these findings, Figure 4 shows different axial velocity RMS distribution between the two burner geometries. While the bluff body burner exhibits a narrow zone of high turbulence level upstream of the IRZ, the non-bluff body displays a much wider high-turbulence zone which extends into the inner shear layer. This is believed to be a key factor in lifted flame stabilization mechanism.

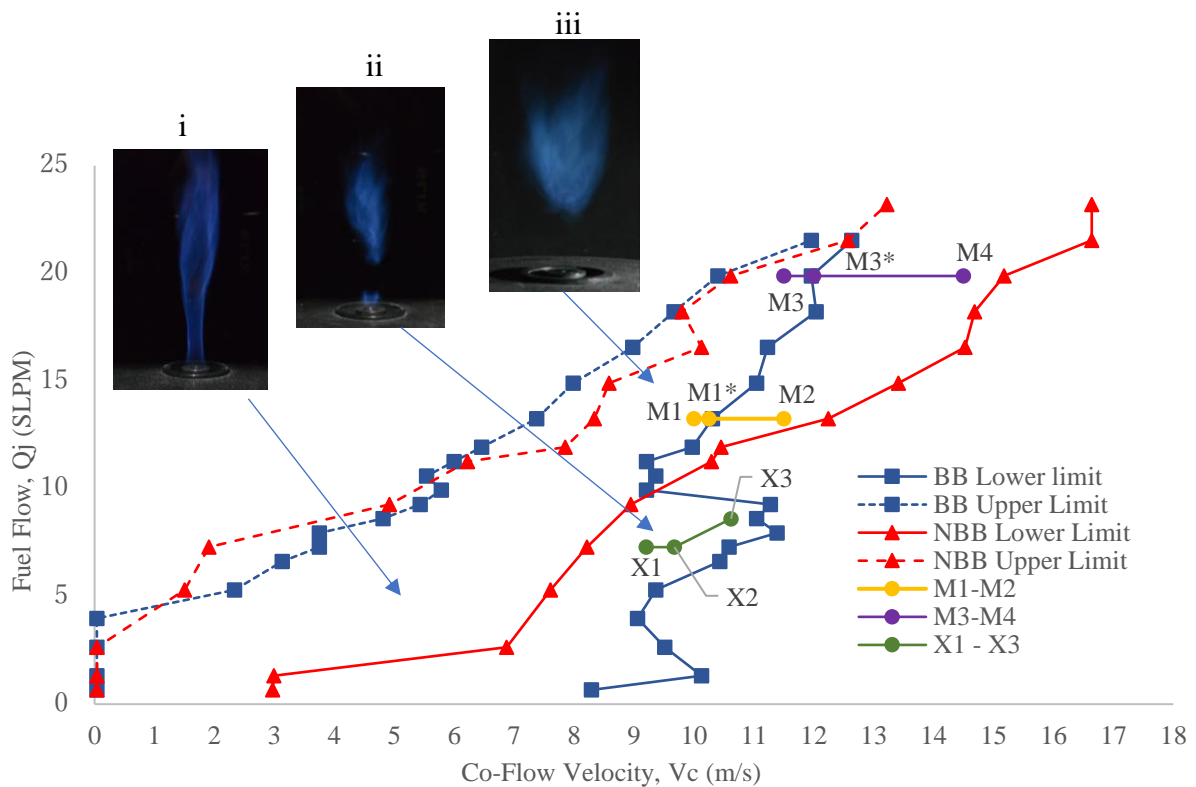


Figure 2. Flammability map of the bluff body (BB) and non-bluff body (NBB) burner configurations. Images of different stable biogas flames are also shown.

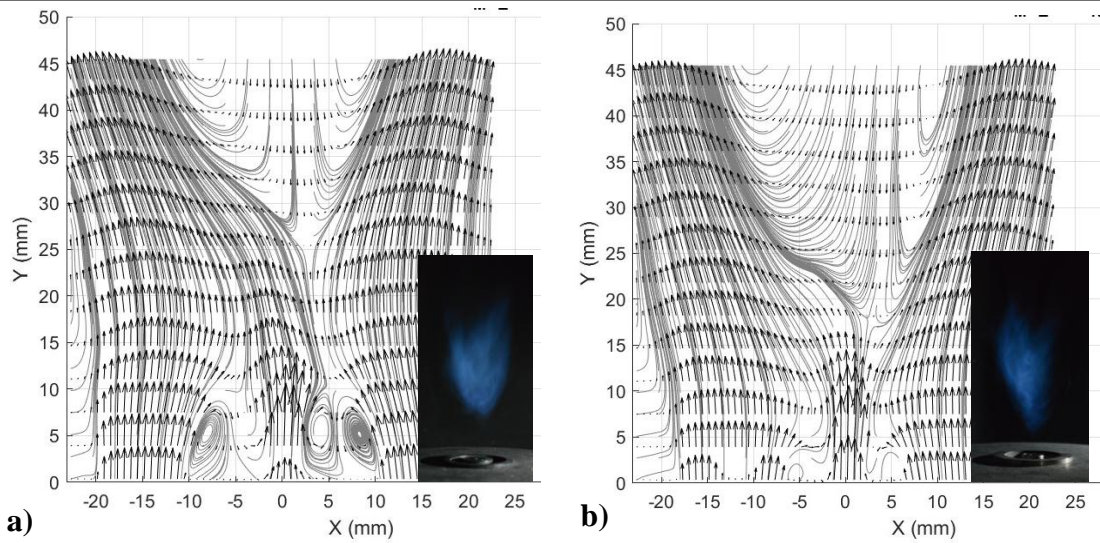


Figure 3. Velocity vector map and streamlines at M1\* point ( $Q_j = 13.25$  SLPM &  $V_c = 10.00$ m/s – see Figure 2). a) bluff body and b) non-bluff body burner.

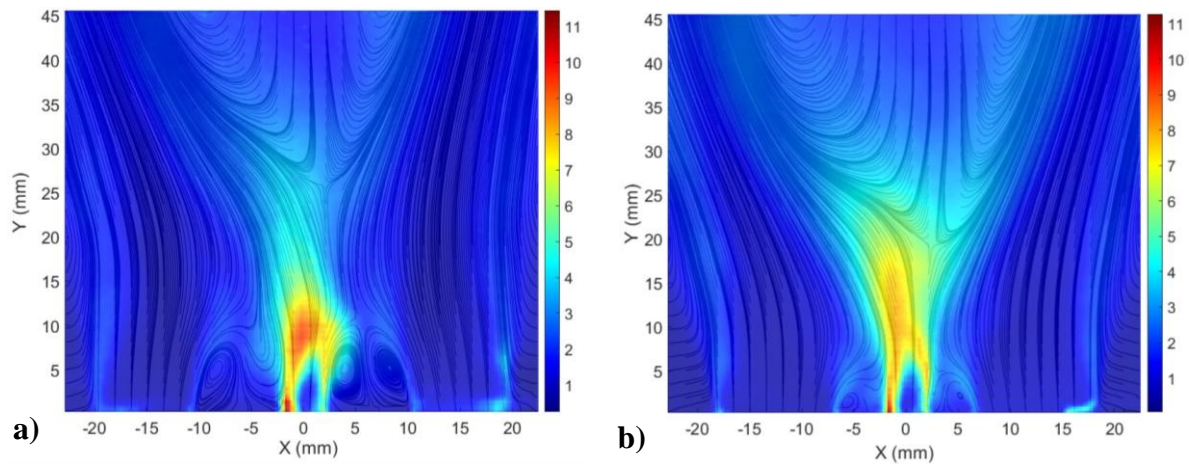


Figure 4. RMS of axial velocity fluctuations and streamlines at M1\* point ( $Q_j = 13.25$  SLPM &  $V_c = 10.00$ m/s – see Figure 2). a) bluff body and b) non-bluff body burner.

### 4 Conclusions

A comparison between the bluff-body and non-bluff burner configurations revealed no significant differences in the upper flame flammability limit. However, the existence of bluff-body induced small recirculation zones closer to the nozzle exit which proved to be important in anchoring the flame and sustaining a stable flame at the lower range of fuel flow rates. This is not the case for the burner with no (or negligible) bluff body. Nevertheless, this bluff body and the presence of relatively small recirculation zones closer to the nozzle exit did not play the same role when increasing both the fuel flow rate and co-airflow velocity where the trend is reversed. That is, the bluff body flame becomes unstable and extinguishes earlier than that of

the non-bluff body burner configuration. These findings (which will be supported by other results not shown here for brevity) highlight the significance of burner geometry in fulfilling specific operational requirements and emphasize the pivotal role of burner design in optimizing flow fields to address the challenges inherent in biogas combustion. This demonstrates the importance of combining fuel burner geometry and swirling co-flow to create flow conditions favorable for stabilizing biogas flame.

## Acknowledgement

This research was supported by the Natural Sciences and Engineering Research Council of Canada (NSERC).

## References

- [1] Saediamiri M., Birouk M., Kozinski J.A. (2016). Enhancing the Stability Limits of Biogas Non-Premixed Flame. *Comb. Science and Technology*. 188:11-12.
- [2] Calbry-Muzyka A. et al. (2022). Biogas composition from agricultural sources and organic fraction of municipal solid waste. *Renewable Energy*. 181:1000-1007
- [3] Jameel M. K. et al. (2024). Biogas: Production, properties, applications, economic and challenges: A review. *Results in Chemistry*. Vol. 7:101549
- [4] C. Hwang et al. (2008). Flame blowout limits of landfill gas mixed fuels in a swirling non-premixed combustor. *Energy & Fuels*. 2933-2940
- [5] Qin W. et al.(2001). Fundamental and Environmental Aspects of Landfill Gas Utilization for Power Generation, *Chemical Engineering Journal*, 157-172
- [6] Leung et al. (2008). The effect of hydrogen addition on biogas non-premixed jet flame stability in a co-flowing air stream. *International journal of Hydrogen Energy*. 3856-3862
- [7] Zhang P., et al. (2021) Comparison of methane combustion mechanisms using laminar burning velocity measurements. *Combustion and Flame*. Vol. 238:111867
- [8] H. Zaidaoui, T. Boushaki, J.C. Sautet, C. Chauveau, B. Sarh, I. Gökalp. (2018). Effects of CO<sub>2</sub> Dilution and O<sub>2</sub> Enrichment on Non-premixed Turbulent CH<sub>4</sub>-Air Flames in a Swirl Burner, *Combust. Sci. Technol.* 190 (5) 784–802.
- [9] Cardona et al. (2013). Laminar burning velocity and interchangeability analysis of biogas/C<sub>3</sub>H<sub>8</sub>, H<sub>2</sub> with normal and oxygen-enriched air. *Journal of Hydrogen Energy*. 7994-8001
- [10] Tong et al. (2018). Effect of the position of a bluff-body on the diffusion flames: A combined experimental and numerical study. *Appl. Therm. Eng.* 131:507-521.
- [11] Khelladi et al. (2021). The Effect of Bluff Body Shape on Flame Stability in a Non-Premixed Hydrogen-Methane-Air Mixture Combustion. *IIETA Vol. 45 No. 5* pp 385-392
- [12] Saediamiri M., Birouk M., Kozinski J.A. (2017). Flame stability limits of low swirl burner – Effect of fuel composition and burner geometry. *Fuel*. 410-422